








Evaluating the impact of the tool and additional fruit cutting on changes of pitted cherries using digital volume correlation with computed tomography

Damian Bańkowski^{1*}, Łukasz Nowakowski², Michał Skrzyniarz²,
Sławomir Błasiak², Piotr Kurp³, Wojciech Depczyński¹, Piotr Młynarczyk¹

¹ Department of Materials Science and Materials Technology, Faculty of Mechatronics and Mechanical Engineering, Kielce University of Technology, al. 1000-lecia P.P. 7, 25-314 Kielce, Poland

² Department of Mechanical Technology and Metrology, Faculty of Mechatronics and Mechanical Engineering, Kielce University of Technology, al. 1000-lecia P.P. 7, 25-314 Kielce, Poland

³ Department of Operational Engineering and Industrial Laser Systems, Faculty of Mechatronics and Mechanical Engineering, Kielce University of Technology, al. 1000-lecia P.P. 7, 25-314 Kielce, Poland

* Corresponding author's e-mail: dbankowski@tu.kielce.pl

ABSTRACT

The paper presents the use of computed tomography examinations to assess the effect of the pitting process on the structure of cherry fruit. The digital volume correlation (DVC) method was used to assess fruit pitting. The aim of this article is to evaluate internal changes in fruit volume, measure deformation, changes in weight, and changes in cherry volume as a result of pitting with various tools. For pitting there are using conventional cross tool head and innovative pitting technology using a rotary knife and a three and four-needle head. The modern VG Studio computer program, designed for tomographic reconstructions, was used for the qualitative analysis of pitting in cherry fruit. The use of modern tools for the analysis of tomographic reconstructions facilitates a range of procedures, including qualitative analysis, measurements, porosity analysis, division into materials, determination of the share of individual materials. Additionally, as evidenced in the present study, digital volume correlation is a valuable tool. Tomographic reconstructions allowed for non-destructive measurements of deformations and damage to the fruit during the pitting process. The voxel displacement tracking method was used to determine the deformations of cherry fruit caused by different pitting technologies. The research results are presented in graphical form, including histograms that taking into account the changes in mass and volume deformations. Furthermore, an analysis of fruit mass losses was performed in order to validate the DVC method. The relative change in fruit volume and mass caused by the pitting process was assessed. The research results indicate that the innovative pitting method with three-needle head is characterized by less deformation and damage to the fruit and a smaller loss of the pericarp volume. The study points that three-needle and four-needle tools result in a reduced degree of fruit degradation in comparison to cross-shaped tools. However, when assessing the exterior surface, it should be noted that additional cutting of the fruit facilitates the removal of the pit and reduces damage to the fruit during the process.

Keywords: X-ray, computed tomography, digital volume correlation, material deformation, non-destructive testing.

INTRODUCTION

From the perspective of the consumer, fruit and vegetable quality characteristics are of paramount importance. Potential consumers of fruit and vegetables focus on visual assessment, which includes size, appearance, shape, color, texture,

and surface defects [1]. Internal characteristics such as firmness, internal defects, or tissue decay are invisible and difficult to assess [1]. Non-destructive testing techniques have been utilised in the agricultural industry for years to determine the ripeness and potential storage life of fruits and vegetables. [2, 3]. The primary objective of

non-destructive testing is the identification and rejection of products exhibiting defects, such as the presence of worms. In the study [4], the authors employed computed tomography to identify internal defects in chestnuts. It has been demonstrated that, by means of CT scans, damaged chestnuts can be detected, as well as the presence of pores, mould, or internal tunnels. External features are the most common factor influencing customer choice, which translates into the economic value of products. Manual testing is time-consuming, costly, destructive process [5], and often lack of objectivity. The assessment of fruit and vegetable characteristics can be facilitated by a range of techniques, including hyperspectral imaging within the visible or near-infrared spectrum [6], Raman imaging, X-ray techniques, computed tomography, magnetic resonance imaging [7], as well as thermal imaging, terahertz imaging, ultrasound imaging, and microwave imaging [8]. In addition, the study [3] used an innovative device for real-time acoustic detection of fruit. The basis of X-ray imaging is the use of contrast resulting from differences in atomic number, density, and thickness of internal structures and tissues, revealing morphological and structural aspects [9] and internal defects [10].

The study [5] focuses on the possibility of processing and analyzing image data. Several machine learning (ML) and deep learning (DL) techniques can be used for this purpose, such as K-nearest neighbors (KNN), artificial neural networks (ANN), support vector machines (SVM), convolutional neural networks (CNN) with transfer learning (TL), generative adversarial networks (GAN), and recurrent neural networks (RNN). These techniques have recently been used for inspection along with spectral data processing [5].

Fruit pitting is the process of extracting the pits from fruits such as cherries, plums, or olives. The process can be done using special equipment such as fruit pitting machines or at home, such as using a hairpin or a fork. A conventional tool for pitting is a cross tool. Following the pitting process, the fruit can be frozen or used to make preserves such as jams, preserves, juices, wines or liqueurs [11]. It is recommended to limit the loss of juices during the process of emptying the pits from the fruit and, consequently, the weight of the pitted fruit. The pitting methods that cause significant damage to the fruit during pit removal result in losses in the volume and mass of the fruit. The optimization of pitting implementation aimed at

reducing the losses in mass and volume of fruit during pitting is expected to result in increased profits for producers and the fruit and vegetable processing industry. It is therefore advisable to indicate the most advantageous method of pitting that allows for effective management of fruit.

A number of studies have so far concentrated on the qualitative description of individual fruits and vegetables through the application of specific non-destructive testing techniques. To the best of the present author's knowledge, no studies have been published on the impact of the pitting process on the external and internal quality of the pitting process. Previous assessments have primarily relied on imaging methodologies, with the surface being the primary focus of evaluation.

The novelty of this article is the 3D qualitative assessment of fruit after pitting with different various tools. In light of the potential to evaluate the internal quality of cherries without compromising the integrity of the fruit itself, the investigative approach encompassed the utilisation of computed tomography and digital volume correlation techniques. These methodologies were employed to ascertain the internal alterations in cherries subsequent to pitting, to quantitatively assess the deformation (i.e. the cavity formed by the pits), and to determine the alterations in cherry weight resulting from pitting. The use of DVC for the analysis of CT images of cherries was used as a way to quantify the effects of mechanical removal of the pit from the fruit. The authors of the study decided to use computer tools to determine the effect of the innovative pitting technique on changes in mass, volume and, above all, volume deformation of the cherry fruit during pitting process.

Cherries are juicy, sweet fruits that are a popular summer treat. They are cultivated on a large scale in Europe, and in Poland, the Masovian Voivodeship is being the largest producer. It is evident that cherries constitute a substantial source of vitamins (A, B, C, K) and minerals (potassium, magnesium, fiber). There are over a thousand known varieties of cherries [12]. There are two main groups of varieties producing fruit called "cockles" (var. juliana) and "cartilages" (var. duracina). The former has soft, juicy flesh, while the latter are more compact, firm and more resistant to transport [13]. The fruit can be categorised into three distinct shades: yellow, red or very dark red, almost black [12]. The fruit of the most popular varieties range in size from medium to very large, with a weight

range of approximately 4 to 11 g [13, 14]. Tomographic examinations use X-ray radiation, which was discovered in 1895 by Wilhelm Roentgen, for non-destructive examinations. Radiographic examinations were very popular in the second half of the 20th century in industry and medicine primarily for the purpose of damage, bone fractures. Performed on classic radiographic film - Radiographs reflected the quality of the objects examined. Thanks to physical phenomena consisting in the absorption of photons by thicker or denser materials, results in a consequent decrease in the number of photons reaching the radiographic film [15, 16]. The technique of research using ionizing radiation consists in archiving X-rays generated from an X-ray tube subsequent to their passing through the tested object on the surface of a digital detector or a conventional radiographic film. As a consequence of the obstruction encountered, X-rays experience a reduction in intensity, thus leading to a decrease in the dose of radiation reaches the receiver [17]. The thickness of the material, its density, and the amount of radiation intensity decreases are all factors that can be used to predict the decrease in intensity [18]. Each material has a characteristic linear attenuation coefficient. Hence, measurements of X-ray intensity subsequent to its transmission the tested object allow for volumetric evaluation. On the other hand, combining of hundreds or even thousands of individual photographs, differing by a small angle of rotation of the tested object allows for spatial visualization of the tested objects. As a result, after the development process, the images on the radiograph were characterized by different degrees of optical density. Industrial computed tomography (CT) is a non-destructive method of examining the internal structure of objects. The tool has the potential to function as an excellent instrument for the purpose of quality control of products and parts. It allows to analysis of objects made of various materials including biological tissues through minerals, ceramics, plastics, to metals and their alloys. It is performed on industrial machines with special software that allows to integration 2D X-ray images into 3D models. Computed tomography in the field of industry, the process of creating a three-dimensional visualization of a detail based on hundreds, or even several thousand X-ray images. Dedicated software combines a series of 2D images into three-dimensional 3D objects.

Grayscale values correspond to the X-ray attenuation of the material components, a function of material density and atomic number and beam

energy [19, 20.]. Composite materials composed of combinations of materials will have different contrasts, which enables identification of the composite components.

X-ray CT enabled three-dimensional visualization and quantification of microstructural changes, including pore number, volume, and equivalent diameter, prior to and after fiber reinforcement. In [21], tomographic studies were used to evaluate the addition of basalt fibres to concrete. The research demonstrated that basalt fibres create a complex spatial stress network, optimizing the pore distribution and delaying the propagation of microcracks. They effectively disperse stress concentrations, mitigate small defects, and refine pore structures, thereby increasing the internal density and resistance to deformation. In [22], X-ray micro-computed tomography was also used to visualize and characterize voids and fibers (length, diameter, and orientation) embedded in concrete. The 3D cracking phenomenon of concrete was analysed using X-ray micro-computed tomography, with the focus being on the formation, development, width, shape, and curvature of the cracking.

X-ray radiation is used in X-ray diffraction studies [23] for quantitative and phase composition, crystal orientation [24] or structure of the tested materials. CT imaging is definitely associated with medical research, as for example in [25] CT imaging was used to examine patients with severe or very severe airflow limitation having a reduced pectoralis muscle area (PMA), which is associated with mortality.

Digital volume correlation (DVC) is a computer tool for measuring and analyzing the deformation of various structures. This tool uses images obtained from computed tomography scans, analyzing 3D models of the examined objects before and after deformation, respectively. Digital volume correlation is an improved tool originally based on two-dimensional digital image correlation (2D-DIC) [26, 27]. Digital image and volume correlation (DIC and DVC) is very commonly used to measure strain and damage in composite materials, as it enables the identification of the directionality and magnitude of internal strains – especially interlaminar and internal damage [28]. Surface displacement photogrammetric techniques can be used to infer damage resulting from non-uniform surface deformation [28]. DVC has the advantage over optical methods due to its ability to perform analyses and measurements of

internal strain. Furthermore, a distinction must be made between in-situ and ex-situ DVC tests. In-situ tests require the installation of a load and temperature measuring device in the CT scanner. In contrast, if the sample is subjected to loading between CT reconstructions, dealing with ex-situ tests. In-situ testing techniques allow for a detailed understanding of the deformation state of materials. Phenomena such as damage development under load are best imaged in-situ, where a constant load/strain can be maintained, excluding any loosening of the specimen [29–32].

The core of the DVC technique is to track (match or register) the same voxel points in volume images of a test object captured in different states by a volume imager [33]. For this purpose, local subvolume-based DVC algorithms and global FEM-based DVC algorithms have been developed in the DIC/DVC modules [34]. In DVC measurements, subvolume size and shape function are two critical user-defined parameters that have a significant impact on the accuracy and precision of detected displacements [35]. The size of the subvolume should be small enough to allow observation of changes relative to the reference subvolume. The shape function should accurately represent the local strain within the target subvolume [34]. In the case of X-ray computed tomography, the pattern is created as a result of changes in the density of the material, such as pores in castings, fragments of particles of other elements inside the tested material [36]. The volume image is divided into sub-volumes of the study, in which the displacement of the pattern is calculated [36].

Too high resolution (reducing the size of a single voxel) generates an increase in file size and requires the use of high computing power of computers, which ultimately translates into analysis time. Therefore, the details of the DVC package

algorithms supplied to programs for analyzing tomographic reconstructions affect the accuracy and precision of measurements of deformation changes in the analyzed reconstructions. In the work of Lorenzo Grassi [37] there is a review of literature on strain measurements on human bone samples at the level of organs and tissues. Four strain measurement methods were used to assess the changes, i.e. strain gauges, fiber Bragg grating sensors, digital image correlation and digital volume correlation. Lorenzo Grassi et al [37] emphasize the advantage of the DVC volumetric method over the analysis of 2D DIC images and the potential application of the method in qualitative research.

MATERIALS

The cherries used for testing were NIMBA (*Prunus avium*) from a single batch (Spain PS/4/OMA1275). They were a relatively large size of about 26–28 mm and medium sensitivity to cracking. The cherries were dark red color and a kidney shape [38]. Figure 1 shows the material for the research.

In order to study the impact of the type of tool and the method of pits removal, the tools shown in Figure 2 were used. The removal of the pits from the cherry fruit was assessed using three different tools: a) cross, b) four-needle and c) three-needle tool. In addition, the pits removal process was compared for all three tools with an additional incision of the fruit with a knife as shown in Figure 2d). The needles used in the study have a diameter of 2 mm. The additional use of a 0.3 mm thick knife results in an incision into the fruit to a depth of approximately 4 mm. The incisions were made automatically by a specially developed pitting machine – Figure 4e). The tools were operated



Figure 1. Cherries of the NIMBA (*Prunus avium*)

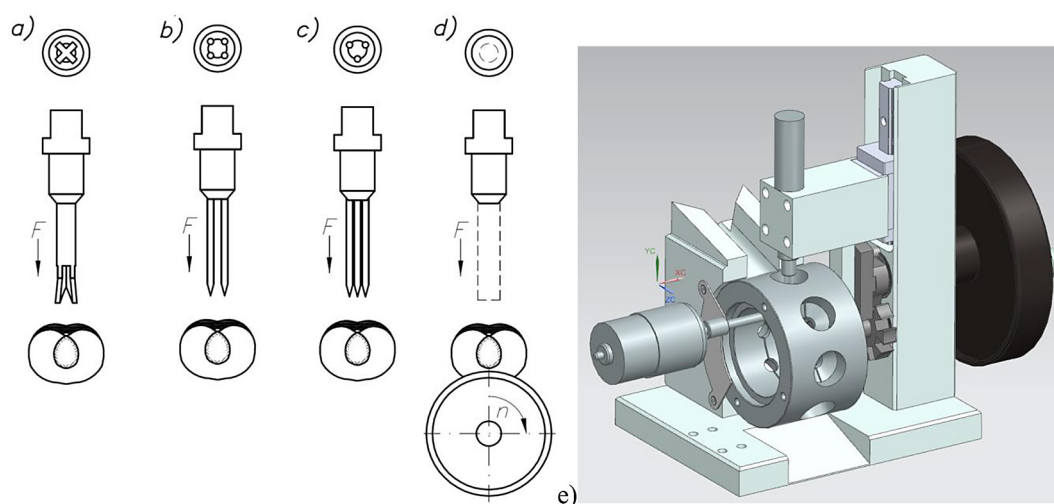


Figure 2. Tools used for pitting cherries: (a) a cross-shaped tool, (b) a four-needle tool, (c) a three-needle tool, (d) a knife for cutting under the fruit to facilitate pits removal, (e) testing station

mechanically without affecting the results of fruit deformation. During the tests, the force exerted by the tool on the fruit was set at 80 N.

CT SCANNING PROCEDURE

Tomographic examinations were performed on a NIKON M2 LES SYSTEM computed tomography scanner (Figure 3). The experiment

employed a 225kV microfocus X-ray tube was used. The VAREX XRD 1611 XP detector with a resolution of 4048×4048 pixels and a pixel size of 0.1 mm was used for archiving. The exposure parameters are presented in Table 1.

The ambient temperature during the test was 18 °C. The tomography test time for a single sample was approximately nine minutes. The volume of each fruit was automatically determined from the histogram, and then the results were calibrated

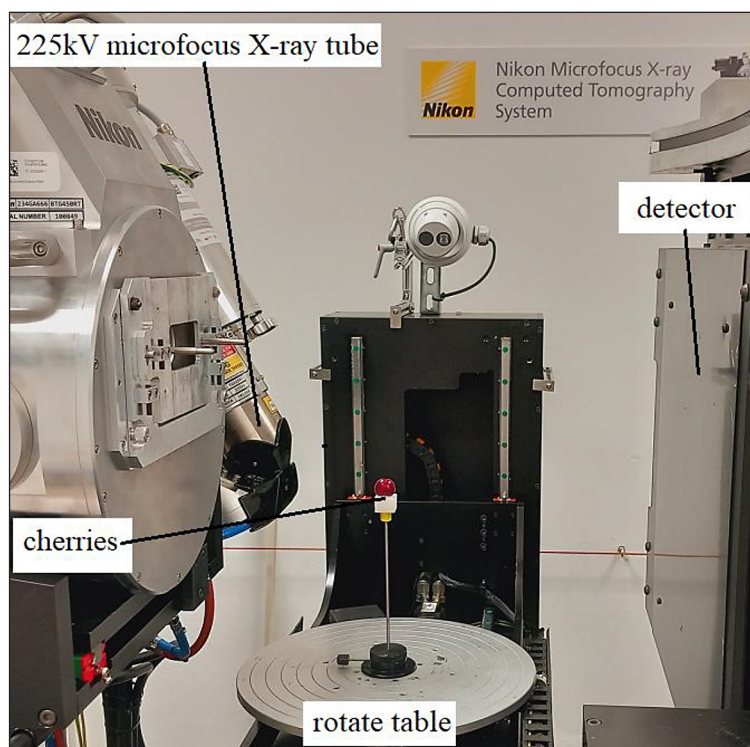


Figure 3. NIKON M2 LES System computed tomography

Table 1. X-ray exposure parameters

Parameter	Value
Voltage	180 kV
Current	310 μ A
Power	55.8 W
Filter	No
Voxel size	25.01 μ m
Projection	1520
Time per projection	354 ms
Distance source-sample	146.62 mm
Distance source-detector	586.33 mm

against a standard. The mass of the samples was measured in each time using a Sartorius CPA124S-0CE scale with a precision of 0.0001 g. Prior to the commencement of the experimental procedure, the scale was subjected to a process of calibration. The samples were weighed approximately 75 hours after harvesting. Samples with a mean weight of 8.61 ± 0.16 g were selected for the tests. Each fruit was weighed before testing. For the pitting analysis, six cherries were tested for each tool, i.e., six for the cross tool without cutting, six for the four-needle tool without cutting, and six for the three-needle tool without cutting. For the purpose of comparison, measurements of fruit weight were taken after pitting with the cross tool, four-needle tool, and three-needle tool with an additional cut. Furthermore, the fruit and pits were weighed again immediately after the pitting process.

IMAGE PROCESSING AND DVC ANALYSIS

The Inspect-X Version V6.8 (Nikon Metrology) program was used to transform 2D radiographic images into 3D tomographic reconstructions. Prior to the creation of a 3D model from the obtained individual 2D radiographic images, a comparison was made between the first and last images to ensure image alignment. Cross-section visualization, analysis, observations, volume measurements of the examined objects, and digital volume correlation were performed in the VG STUDIO MAX version 2022.4 program from Volume Graphics software.

Digital Volume Correlation is a module in VG STUDIO MAX that allows to the calculation of the displacement between the initial and deformed volumes. The DVC module for VGSTUDIO MAX, calculate the movement of each voxel

from one volume to another, to analyze in-situ tests or part deformations based on actual component loads. The software measures local displacement and strain tensors, visualizes deformations and movements using arrows or displacement lines, and maps the results to finite element (FE) meshes to verify simulations [33].

In the study, cherry fruits in their original state – containing pits – were subjected to tomographic examination. The items were then subjected to pitted: 6 pieces with a classic cross-shaped tool, 6 pieces with a three-needle tool, and 6 pieces with a four-needle tool. Tomographic examinations were performed again. The obtained 3D models were then subjected to analysis using DVC. Based on DVC, it is possible to graphically determine the changes in fruit deformation in accordance with the tool employed for the pitting process. Tomographic analysis facilitates the dimensional quantification of the channels that are formed subsequent to the pitting process. In addition, the study used an innovative additional cutting of the fruit to facilitate the removal of the pit. The innovative technological solution developed allows for reducing the forces necessary to extract the pit [11] from the cherry fruit. Tomography of the fruit was performed analogously, first on the whole fruit and then after cutting and pitting with various tools. Maximum material displacements were measured for the purpose of DVC analysis. The mean maximum material displacements for a series of a given pitting tool without cutting were compared to pitting with cutting.

The measurements were performed ex-situ by analyzing the whole fruit. The initial volume of cherries prior to pitting was selected as the object before deformation. A comparison was made between the volumes of cherries after pitting. The “best fit” method was used to align volumes. For the DVC analysis, the resolution was not modified and corresponded to the original resolution of the CT reconstruction, 25 μ m resample voxel size. The local non-linear transformation type was used. Non-linear deformation is described by a non-uniform displacement field. The field is defined by displacement vectors on a regular grid of control points. The field is interpolated between the control points, using cubic b-splines. The control point spacing was set at 0.4, which corresponded to 16 voxels. Normalized cross correlation was used as a similarity measure. The number of iterations was set at 500. The volume of the fruit was determined on the basis of tomographic reconstructions, before

the pitting process and after pitting, both the fruit and the pits. Equation 1 describes the changes in volume during the process of pitting.

$$\Delta V = V_1 - V_2 - V_p \quad (1)$$

where: V_1 – volume of cherries before pitting;
 V_2 – volume of cherries after pitting; V_p – volume of pits after pitting.

The difference in the volume of the fruit prior and volume of the fruit and pit after pitting enables the calculation of the volume loss depending on the type of tool used for pitting, as well as the effect of an additional incision in the fruit. The use of computed tomography to illustrate the internal changes occurring as a result of removing the pits from the fruit is an excellent example of the use of advanced technology to analyse the effects of a process on a subject. Additionally, numerical data in the form of a reduction in the actual volume of

the fruit show which of the pitting methods causes the least damage least during pitting.

RESULTS AND DISCUSSION

Non-destructive testing, including radiographic testing [39], is particularly well-suited to quality testing and detecting internal changes in materials. As confirmed in [40], the implementation of non-destructive testing during operational procedures allows the technical inspection of materials. Based on the volume data of the tested fruits obtained from tomographic reconstructions of the fruits before and after pitting, graphs of the average fruit volume loss depending on the type of tool used to remove the pits were drawn up as shown in Figure 4. The mean values were determined based on measurements of volume loss for

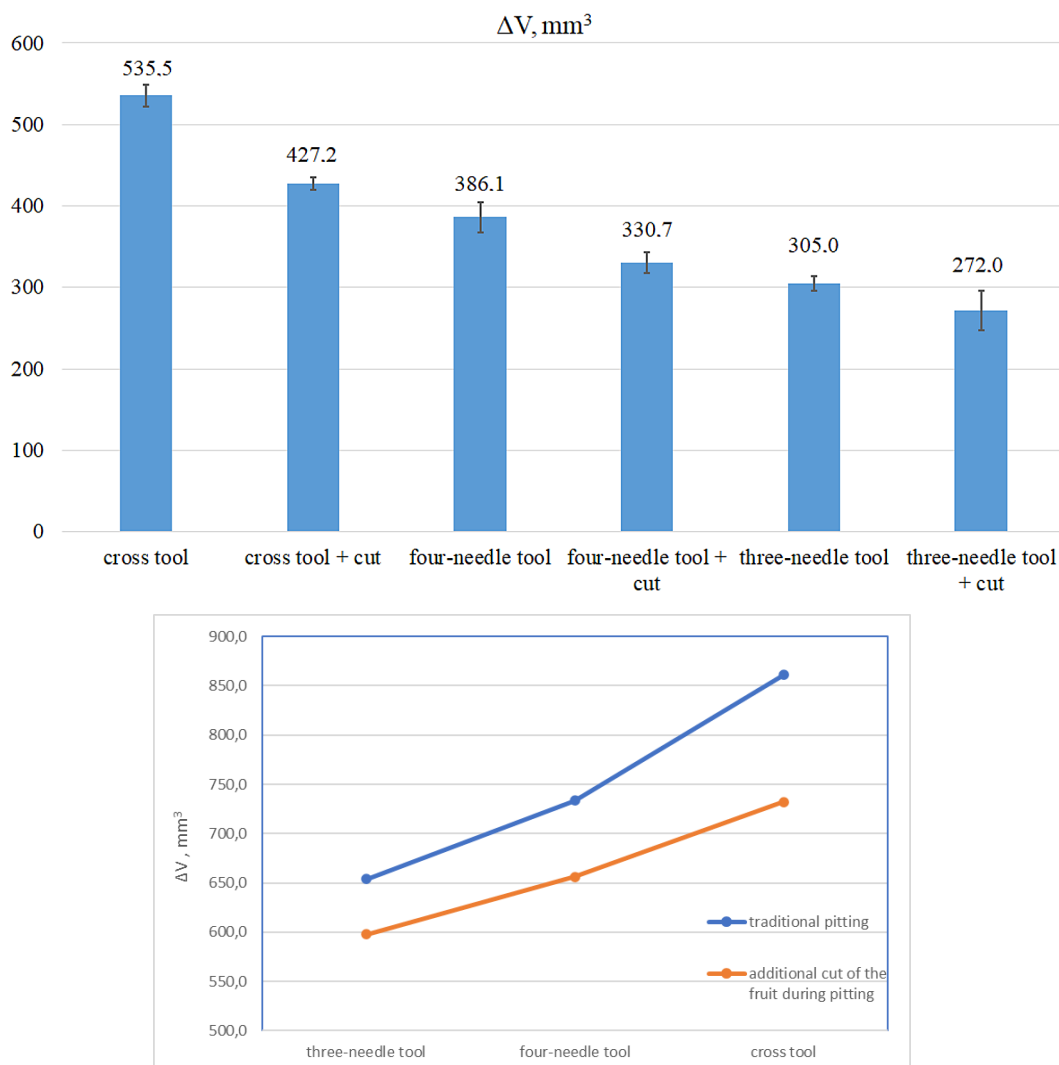


Figure 4. Graph of mean volume loss of the fruit due to pitting, depending on the pitting tool and method

six fruits pitted with a specific tool. Furthermore, the graph shows the effect of an additional cut in the fruit prior pitting.

In turn, the data of mean fruit mass measurements prior and after pitting allowed for the preparation of graphs of mass losses depending on the type of tool used to remove the pits, as shown in Figure 5. The mean values were determined based on formula No. (1) of mass loss measurements for six fruits pitted with a specific tool. In addition, the graph illustrates the effect of an additional cut in the fruit prior to pitting.

Based on the graphs, it can be stated that the largest losses in volume and mass of the fruit were observed in the case of pitting with a classic cross tool. The use of a four-needle tool for pitting reduces the volume losses by approximately 150 mm³ (1.8%) and mass losses by around 0.02 g (7.5%) compared to the cross tool. Reducing the number of needles to three allows for directional removal of the pits from the fruit, while causing

less impact on the fruit itself when compared to the use of a four-needle or cross tool. As a result of using a three-needle tool, an average of about 230 mm³ (2.8 %) smaller volume loss and about 0.046 g (16.9%) smaller mass loss of the fruit during pitting was obtained compared to the classic cross tool. In addition, analysis of graphs 4 and 5 indicate that the use of a fruit cut prior to the pitting process causes an additional reduction in volume loss during pitting from 33 mm³ (0.4%) for the three-needle head to 108 mm³ (1.3%) for the cross head.

In order to visualize the internal changes of fruits pitted using different methods, Figures 6–8 present tomographic visualizations of cross-sections of classically pitted fruits, whole fruits and fruit cut with the use of additional fruit cutting. The figures also show cross-sections near the center of the fruit with the maximum dimensions of voids after the pits has left the fruit during pitting.

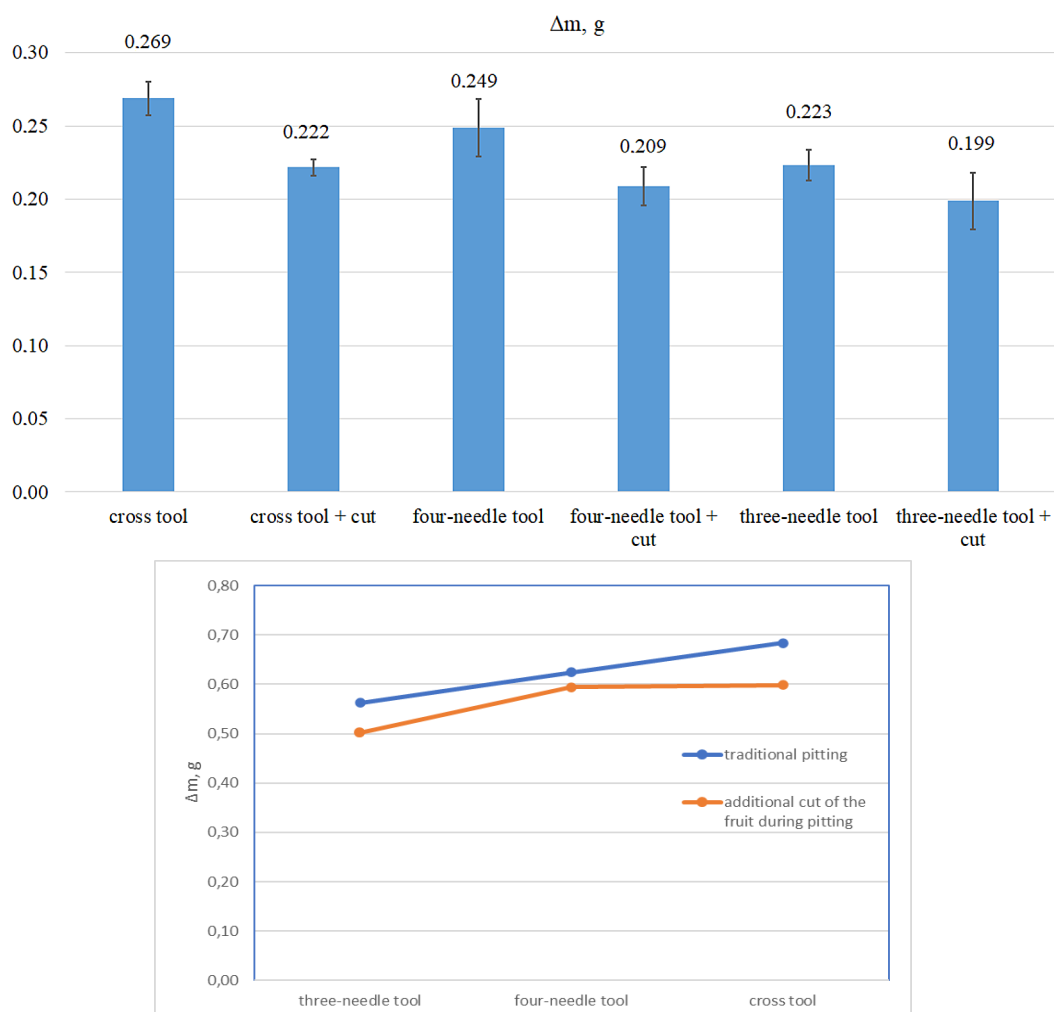


Figure 5. Graph of mean mass loss of the fruit due to pitting, depending on the pitting tool and method

As illustrated in Figures 6 to 8a cross-sections of 3D models of tomographic reconstructions of cherry fruits after pitting with a classic cross tool, a four-needle head, and a three-needle head, respectively, are presented. In addition, Figures 6–8b illustrate cross-sections of 3D models following the induction of pitting and prior cutting of the fruit.

Subsequent to the removal of the pits, measurements were taken of the holes that had been created. As illustrated in Table 2, the mean values from six fruits pitted with each tool are presented. In addition, measurements of mean diameter were taken of two perpendicular diagonals of the holes obtained after pitting. The table also contains the average maximum displacement values for specific tools, generated during DVC analyses.

Computed tomography allows for measuring the length, volume, and analysis of the occurrence of pit voids. The reconstructions were used

to measure the maximum dimensions of the channels in the central part of the fruit following pitting. Comparing the obtained tomographic reconstructions of the cherry fruit after the process of pitting with a three-needle spearhead and a classic spearhead with a cross-shaped tool, can observe an approximate magnitude 0.4 mm greater destruction of the pericarp in the case of pitting with classic cross-shaped tools. The obtained medium values confirm. The use of a cross-shaped tool during the pitting process resulted in pits with an average diameter of 8.3 mm. Subsequent to the replacement of the pitting tool with a four-needle head, the hole of pits exhibited a mean diameter of 8.1 mm, whilst the three-needle tool yielded a mean diameter of 7.9 mm. An additional cutting in the cherry during pitting reduces the pit canal to an average diameter of approximately 7.99 mm for the cross tool, 7.74 mm for the four-needle

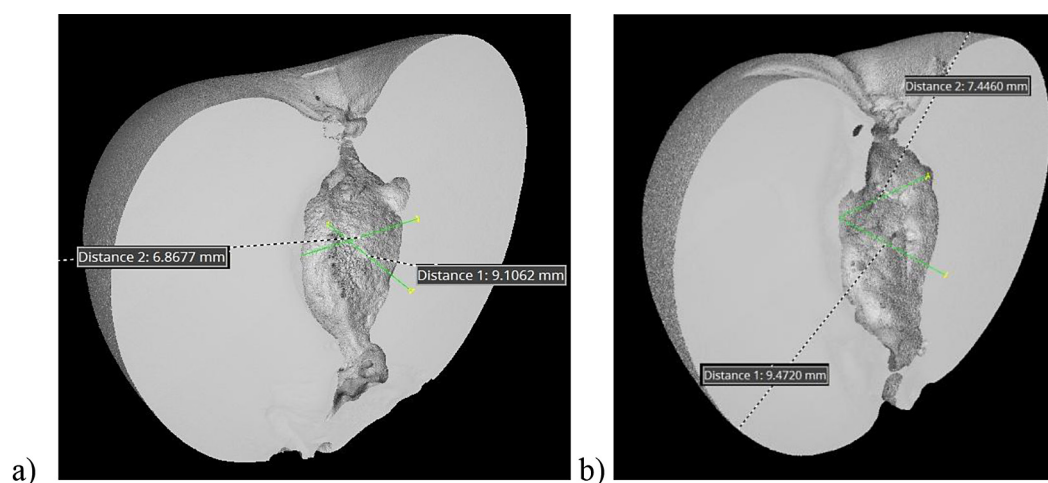


Figure 6. View of the 3D CT model of a cherry fruit after pitting with a classic cross-shaped tool (a) without undercutting the fruit, (b) with the fruit cut before pitting

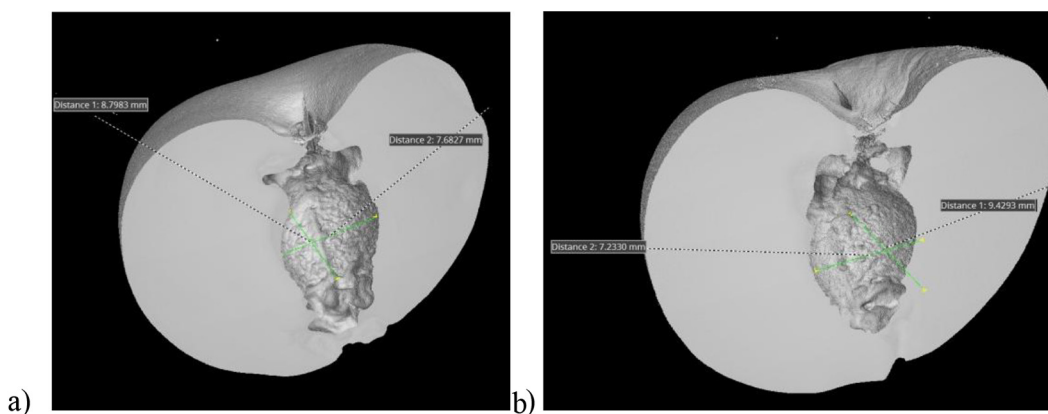


Figure 7. View of the 3D CT model of a cherry fruit after pitting with a four-needle tool (a) without undercutting the fruit, (b) with the fruit cut before pitting

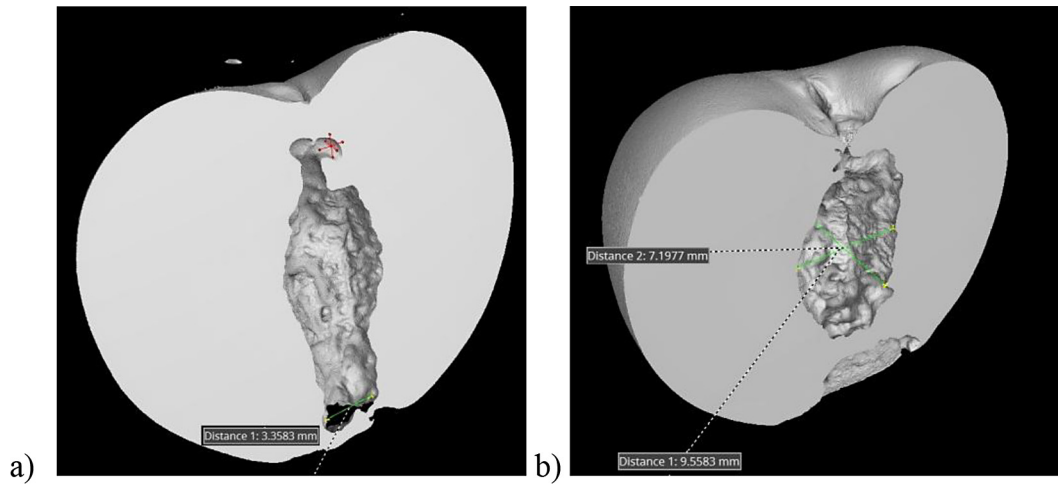


Figure 8. View of the 3D CT model of a cherry fruit after pitting with a three-needle head (a) without undercutting the fruit, (b) with the fruit cut before pitting

Table 2. Mean diameter (d_{av}) and maximum material displacement (ϵ_{max}) after pitting

Type of tool for pitting	d_{av} , mm	ϵ_{max} , mm
Cross tool	8.3132	5.9073
Cross tool + cut	7.9870	5.3607
Four-needle tool	8.0774	4.8595
Four-needle tool + cut	7.7405	4.1161
Three-needle tool	7.8780	4.8076
Three-needle tool + cut	7.6021	4.1004

tool, and 7.60 mm for the three-needle tool. Figures 9–11 present graphical representations of digital volume correlation analyses of sweet cherries of the NIMBA (*Prunus avium*) fruits following pitting with a classic cross-shaped tool, a four-needle head and a three-needle head. In addition, Figures 9–11b illustrate cross-sections of

3D models following the pitting process and prior cutting of the fruit. Tomographic reconstructions of sweet cherries before pitting were selected as the base material for analysis, while reconstructions of the same fruits after pitting were selected after deformation.

DVC from CT images enables the acquisition of 3D deformation and damage measurements that are practically impossible to achieve using other characterization techniques [28]. The use of DVC enables the identification of subsurface damage [28] and the characterization of internal tissues [9]. As illustrated on Figure 9–11, graphical visualizations of internal changes in the fruits – present the magnitude of displacements inside the fruits. The VG Studio software determines the maximum displacement of the material post pitting in comparison to the fruit prior to pitting. The

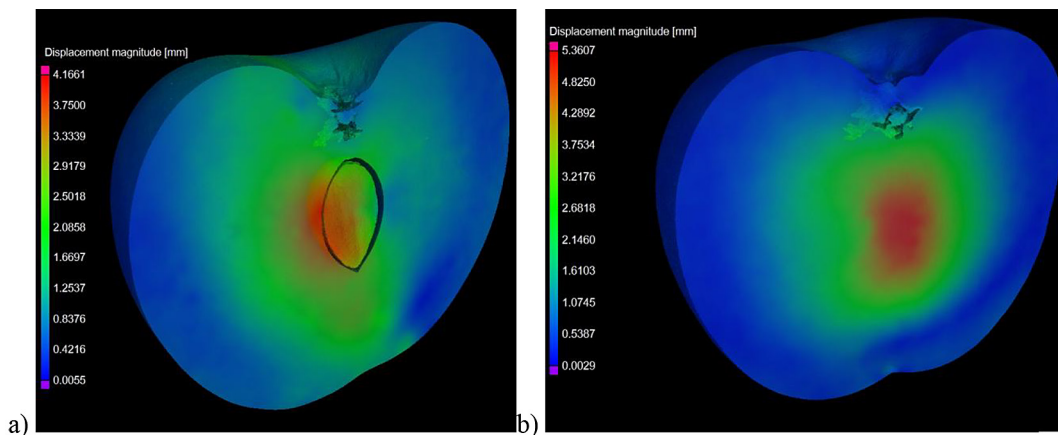


Figure 9. View of the 3D digital volume correlation model of a cherry fruit after pitting with a classic cross-shaped tool (a) without undercutting the fruit, (b) with the fruit cut before pitting

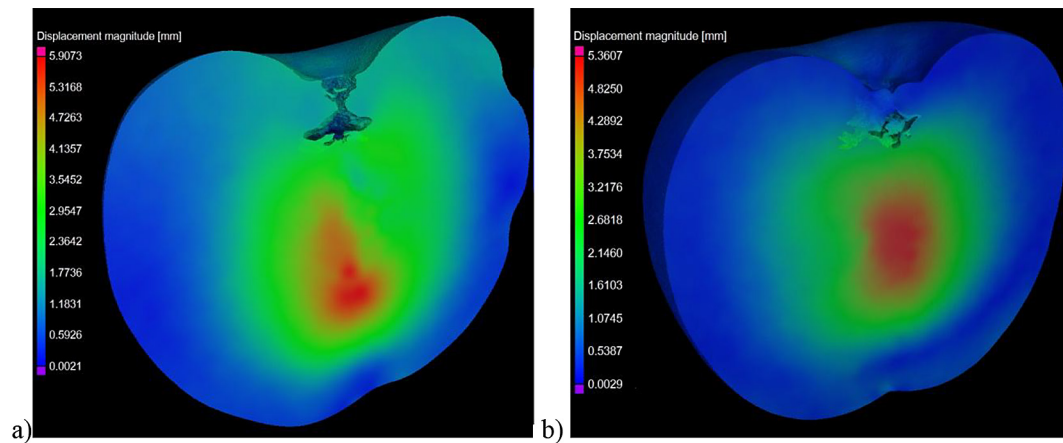


Figure 10. View of the 3D digital volume correlation a cherry fruit after pitting with a four-needle tool (a) without undercutting the fruit, (b) with the fruit cut before pitting

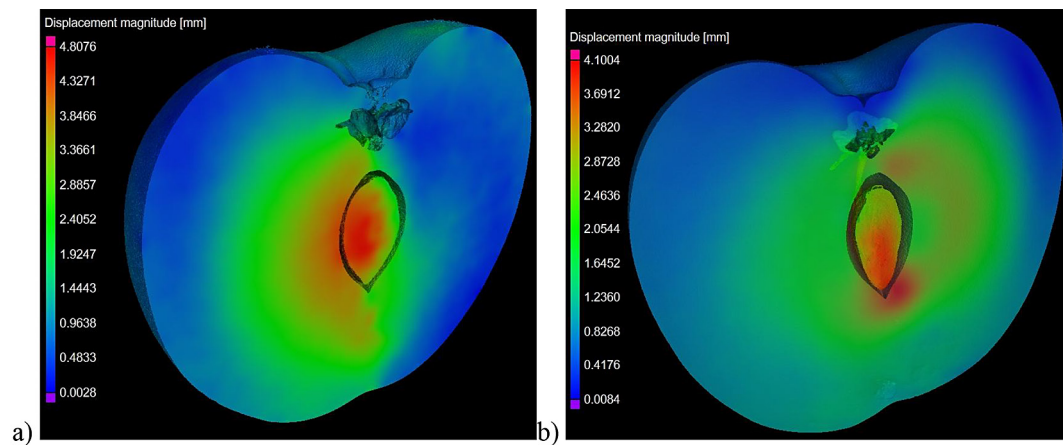


Figure 11. View of the 3D digital volume correlation of a cherry fruit after pitting with a three-needle head (a) without undercutting the fruit, (b) with the fruit cut before pitting

mean values of the maximum material displacements from 6 fruits pitted using each method are summarized in Table 2.

The largest changes inside the fruit, with a maximum diameter of 5.91 mm can be observed in the case of pitting with a classic cross tool. When pitting with a four-needle tool, a maximum material displacement of 4.86 mm can be observed. In contrast, when pitting with a three-needle tool results in a maximum material displacement of 4.81 mm is attained. Replacing a large-surface tool - a cross with needle tools causes smaller deformations inside the fruit at the point of entry of the tool into the workpiece. An additional cut in the fruit prior pitting causes a reduction in the deformation field at the point of exit of the pits from the fruit. For the cross tool, a reduction in the maximum material displacement to 5.36 mm can be observed, while for the

four-needle and three-needle tools, the reduction is 4.2 and 4.10, respectively. The aforementioned factors ultimately result in diminished fruit mass loss during pitting. This work will contribute to obtaining more accurate information about the pitting process. Furthermore, it is predicted that new knowledge about the mechanism of the pitting process and the results of the tool's impact on fruit weight and volume loss during pitting. Supporting fruit selection techniques with artificial intelligence [1] improve the quality of products offered to customers.

CONCLUSIONS

DVC studies have been shown to create significant opportunities for the application in other studies of composite, biological materials or

strength testing. The findings of the conducted studies provide evidence to support this claim:

The lowest volume losses were observed during pitting with a three-needle head with the fruit undercut, followed by the four-needle head, with the greatest losses occurring for the cross tool. The substitution of the cross-shaped pitting tool with a three-needle tool has been demonstrated to reduce the volume loss of pitted fruit by approximately 43%. However, the use of an additional cutting implement and a three-needle tool, in comparison with conventional pitting utilising a cross-shaped tool, has been demonstrated to result in a volume reduction of approximately 49%.

The findings of the mass loss studies confirm the results obtained from tomographic analyses and digital volume correlation. The most substantial average mass losses were observed for pitting with a cross tool, amounting to approximately 0.27 g. Substituting the pitting tool with a three-needle head resulted in a reduction of fruit mass losses by approximately 17%, and the combination of an additional cut and a three-needle head led to a further reduction of 26%.

In order to limit the deformation of the material, it is advisable to replace the classic cross tools for pitting with a four-needle or three-needle tool. Pitting with a four-needle tool results in smaller holes around the pit with an average diameter of 0.24 mm, while pitting with a three-needle tool results in smaller channels around the pit with an average diameter of 0.44 mm compared to a cross tool. Furthermore, an additional cut of the cherry fruit before pitting reduces the average diameter of the pit channel by 0.33 mm for the cross tool, 0.34 mm for the four-needle tool, and 0.28 mm for the three-needle tool.

Digital image correlation is a method of measuring maximum material displacement during pitting. The maximum material displacement achieved was greatest for the cross tool, reaching an approximate value of 8.31 mm. The replacement of the pitting head with a four-needle tool resulted in a reduction of maximum material displacement by 0.13 mm, while utilising a three-needle tool led to a decrease of 0.43 mm. Moreover, the additional cut reduced the maximum material displacement by an average of approximately 0.3 mm for each method.

The study confirms the hypothesis that substituting cross tools with a three-needle pitting tool and creating an additional incision in the fruit will minimize waste during the pitting process.

The utilization of tomographic testing and digital image analysis in a range of applications, including those requiring high-quality materials, such as in the military and aviation industries, is a testament to their versatility and efficacy.

It is advisable that analogous research be expanded to encompass fruits and vegetables that are particularly vulnerable to damage during pitting processes. Subsequent research will concentrate on cherries, which are comparable in size to sweet cherries but are more vulnerable to damage.

Acknowledgements

The research reported herein was supported by a grant from The Agency for Restructuring and Modernisation of Agriculture (ARMA) involving funds of European Agricultural Fund for Rural Development (EAFRD) for the years 2014-2020 under action 16 “Cooperation”. Grant title: “Technological, process and product innovation in pitting cherries in such a way that the structure of the fruit is disturbed as little as possible in cooperation with the Kielce University of Technology”, contract number: 00028.DDD.6509.00125.2019.13.

REFERENCES

1. Tian, S., Xu, H. Nondestructive methods for the quality assessment of fruits and vegetables considering their physical and biological variability. *Food Eng Rev* 2022; 14, 380–407. <https://doi.org/10.1007/s12393-021-09300-0>
2. Kumari, P., Ahmad, M. F., Mir, H. (2018) Non-destructive quality evaluation by sensing maturity and ripening of fruits and vegetables. *Journal of Postharvest Technology*. 2018; 6(2).
3. Chen, N., Liu, Z., Zhang, T., Lai, O., Zhang, J., Wei, X., Liu, Y. Research on prediction of yellow flesh peach firmness using a novel acoustic real-time detection device and Vis/NIR technology, *LWT*, 2024; 209, 116772. <https://doi.org/10.1016/j.lwt.2024.116772>
4. Wang, J., Lu, Z., Xiao, X., Xu, M., Lin, Y., Dai, H., Liu, X., Pi, F., Han, D. Non-destructive determination of internal defects in chestnut (*Castanea mollissima*) during postharvest storage using X-ray computed tomography, *Postharvest Biology and Technology*, 2023; 196, 112185. <https://doi.org/10.1016/j.postharvbio.2022.112185>
5. Akter, T., Bhattacharya, T., Kim, J.-H., Kim, M. S., Baek, I., Chan, D. E., Cho, B.-K. A comprehensive

- review of external quality measurements of fruits and vegetables using nondestructive sensing technologies, *Journal of Agriculture and Food Research*, 2024; 15, 101068. <https://doi.org/10.1016/j.jafr.2024.101068>
6. Anthony, B. M. Sterle, D. G., Minas, I. S. Robust non-destructive individual cultivar models allow for accurate peach fruit quality and maturity assessment following customization in phenotypically similar cultivars, *Postharvest Biology and Technology*, 2023; 195, 112148, <https://doi.org/10.1016/j.postharvbio.2022.112148>
7. Lan, W., Hui, X., Nicolai, B., Verboven, P., Qin, J., Renard, C. M. G. C., Pan, L. (2024). Visualizing the structural and chemical heterogeneity of fruit and vegetables using advanced imaging techniques: fundamentals, instrumental aspects, applications and future perspectives. *Critical Reviews in Food Science and Nutrition*, 65(21), 4147–4171. <https://doi.org/10.1080/10408398.2024.2384650>
8. Li, L., Jia, X., Fan, K. (2024). Recent advance in nondestructive imaging technology for detecting quality of fruits and vegetables: a review. *Critical Reviews in Food Science and Nutrition*, 1–19. <https://doi.org/10.1080/10408398.2024.2404639>
9. Hernández-Sánchez, N., Moreda, G., Herretero-Langreo, A., Melado-Herreros, Á. Assessment of Internal and External Quality of Fruits and Vegetables. In: Sozer, N. (eds) *Imaging Technologies and Data Processing for Food Engineers*. Food Engineering Series. Springer, Cham. 2016. https://doi.org/10.1007/978-3-319-24735-9_9
10. Nicolai, B., Ketelaere, B. De., Dizon, A., Wouters, N., Postelmans, A., Saeys, W., Van de Looverbosch, T., Verboven, P., Hertog, M. L.A.T.M. Chapter 14 - Nondestructive evaluation: detection of external and internal attributes frequently associated with quality and damage, Editor(s): Florkowski, W. J., Banks, N. H., Shewfelt, R. L., Prussia, S. E. *Postharvest Handling (Fourth Edition)*, Academic Press, 2022; 399–433. <https://doi.org/10.1016/B978-0-12-822845-6.00014-2>
11. Nowakowski L., Kurp P., Skrzyniarz M., Błasiak S., Depczyński W. Pits transporting system from pitter fruit machine - case study. *Communications*. 2024; 26(2), B128–B134. <https://doi.org/10.26552/com.C.2024.025>
12. Szweykowska A., Szweykowski J. (red.): *Słownik botaniczny (Botanical dictionary)*. 2nd edition, revised and supplemented. Warsaw: Wiedza Powszechna, 2003: 992. (in Polish).
13. Pieniążek S.A. *Sadownictwo (Orchardry)*. Warsaw: Państwowe Wydawnictwo Rolnicze i Leśne, 1988; 54, 105–110. (in Polish).
14. Głowacka A., Rozpara A. *Ilustrowany katalog odmian czereśni (Illustrated catalogue of cherry varieties)*. Institute of Horticulture, Skierniewice 2013, (in Polish).
15. Depczynski W. P., Bankowski D., Mlynarczyk P. S. Computed tomography and scanning electron microscopy analysis of a friction stir welded Al-Cu joint. *Archives Of Foundry Engineering*. 2023; 23(4), 5–71. <https://doi.org/10.24425/afe.2023.146680>
16. Bańkowski D., Mlynarczyk P., Spadło S., Sójka R., Klamczyński K. Tomographic testing of alnico alloys. *Proceedings 31 International Conference on Metallurgy and Materials*. 2022; 675–681. <https://doi.org/10.37904/metal.2022.4507>
17. Bańkowski D., Mlynarczyk P. Visual testing of castings defects after vibratory machining. *Archives of Foundry Engineering*. 2020; 4/2020, 72–7. <https://doi.org/10.24425/afe.2020.133350>
18. Bańkowski D.; Kiljan A.; Hlaváčová I.M.; Mlynarczyk P. Influence of Selected Factors of Vibratory Work Hardening Machining on the Properties of CuZn30 Brass. *Materials*. 2024; 17, 5913. <https://doi.org/10.3390/ma17235913>
19. Hermanek P., Rathore J. S., Aloisi V., Carmignato S. Principles of X-ray computed tomography. In: *Industrial X-ray computed tomography*. 2017; 25–67. http://dx.doi.org/10.1007/978-3-319-59573-3_2
20. Villarraga-Gómez H., Herazo E. L., Smith S. T. X-ray computed tomography: from medical imaging to dimensional metrology. *Precis Eng* 2019; 60: 544–69. <http://dx.doi.org/10.1016/j.precisioneng.2019.06.007>
21. Kong L., Xu J. R., Yang H. B., Wu P. F., Li X. Y., Ma D. Y., Wang Z. L., Ren D. Y., Ai C. F. Enhancing crack resistance in basalt fiber asphalt mixtures: a full-field time-domain investigation of stress distribution and pore structure optimization. *International Journal of Pavement Engineering*. 2025; 26(1). <https://doi.org/10.1080/10298436.2025.2460746>
22. Żorawski W, Vicen M, Trelka-Druzic A i in. Mikrostruktura i właściwości mechaniczne natryskiwanej na zimno powłoki amorficznej. *Czasopismo Badawcze Postępów Nauki i Technologii*. 2024; 18(8): 73–85. <https://doi.org/10.12913/22998624/193479>
23. Gancarczyk K., Albrecht R., Kawalec M., et al. The effect of re content on microstructure and creep resistance of single crystal castings made of nickel-based superalloys. *Advances in Science and Technology Research Journal*. 2024; 18(1): 291–305. <https://doi.org/10.12913/22998624/178463>
24. Skarzyski L., Suchorzewski J. Mechanical and fracture properties of concrete reinforced with recycled and industrial steel fibers using Digital Image Correlation technique and X-ray micro computed tomography. *Construction And Building Materials*. 2018; 183, 283–299, <https://doi.org/10.1016/j.conbuildmat.2018.06.182>
25. Zhou K., Wu F., Zhao N., Zheng Y., Deng Z., Yang

- H., Wen X., Xiao S., Yang C., Chen S. Association of pectoralis muscle area on computed tomography with airflow limitation severity and respiratory outcomes in COPD: A population-based prospective cohort study. *Pulmonology*. 2023; 31(1). <https://doi.org/10.1016/j.pulmoe.2023.02.004>
26. Perilli, B. C. R. E., Reynolds, K. J. Application of the digital volume correlation technique for the measurement of displacement and strain fields in bone: A literature review. *Journal of Biomechanics*. 2014; 47(5), 923–934. <https://doi.org/10.1016/j.jbiomech.2014.01.001>
27. Shao X., Dai X., He X. Noise robustness and parallel computation of the inverse compositional Gauss–Newton algorithm in digital image correlation. *Optics and Lasers in Engineering*. 2015; 71, 9–19. <https://doi.org/10.1016/j.optlaseng.2015.03.005>
28. Holmes J., Sommacal S., Das R., Stachurski Z., Compston P. Digital image and volume correlation for deformation and damage characterisation of fibre-reinforced composites: A review, *Composite Structures*. 2023; 315, 116994. <https://doi.org/10.1016/j.compstruct.2023.116994>
29. Castaneda N., Wisner B., Cuadra J., Amini S., Kontsos A. Investigation of the Z-binder role in progressive damage of 3D woven composites. *Composites A*. 2017; 98, 76–89. <https://doi.org/10.1016/j.compositesa.2016.11.022>
30. Mao L., Liu H., Zhu Y., Zhu Z., Guo R., Chiang F. 3D strain mapping of opaque materials using an improved digital volumetric speckle photography technique with X-Ray microtomography. *Appl Sci*. 2019; 9(7). <https://doi.org/10.3390/app9071418>
31. Wang B., Pan B., Lubineau G. Morphological evolution and internal strain mapping of pomelo peel using X-ray computed tomography and digital volume correlation. *Mater Des*. 2018; 137, 305–315. <https://doi.org/10.1016/j.matdes.2017.10.038>
32. Forna-Kreutzer J. P., Ell J., Barnard H., Pirzada T. J., Ritchie R. O., Liu D. Full-field characterisation of oxide-oxide ceramic-matrix composites using X-ray computed micro-tomography and digital volume correlation under load at high temperatures. *Mater Des*. 2021; 208, 109899. <https://doi.org/10.1016/j.matdes.2021.109899>
33. <https://volumegraphics.hexagon.com/en/products/add-on-modules/digital-volume-correlation.html>
34. Pan B., Wang B. Some recent advances in digital volume correlation, *Optics and Lasers in Engineering*. 2020; 135, 106189. <https://doi.org/10.1016/j.optlaseng.2020.106189>
35. Bay B. K. Methods and applications of digital volume correlation. *The Journal of Strain Analysis for Engineering Design*. 2008; 43(8), 745–760. <https://doi.org/10.1243/03093247JSA436>
36. <https://www.smart-piv.com/en/applications/materials-testing/digital-volume-correlation-dvc>
37. Grassi L., Isaksson H. Extracting accurate strain measurements in bone mechanics: A critical review of current methods. *Journal of the Mechanical Behavior of Biomedical Materials*. 2015; 50, 43–54. <https://doi.org/10.1016/j.jmbbm.2015.06.006>
38. <https://www.dalival.com/cerises/nimba-pol>
39. Konieczny J., Labisz K., Majchrzak A., Atapek S. H. Application of the nondestructive and destructive research to disclose identification marks on vehicles. *Advances in Science and Technology Research Journal*. 2025; 19(4), 280–293. <https://doi.org/10.12913/22998624/200481>
40. Malec M., Cieplak T., Walczuk S. Non-destructive tests of lock tongues used IN ATR-72 aircraft landing gear based on magnetic method. *Advances in Science and Technology Research Journal*. 2013; 7(20), 23–28. <https://doi.org/10.5604/20804075.1073049>